2007 IEEE International Conference on
Robotics and Automation
Roma, Italy, 10-14 April 2007

Minimum Wheel-Rotation Paths for Differential Drive Mobile Robots Among Piecewise Smooth Obstacles

Hamidreza Chitsaz
Department of Computer Science
University of Illinois at Urbana-Champaign
chitsaz@cs.uiuc.edu

Steven M. LaValle
Department of Computer Science
University of Illinois at Urbana-Champaign
lavalle@cs.uiuc.edu

***Abstract*— Computing optimal paths for mobile robots is an interesting and important problem. This paper presents a method to compute the shortest path for a differential-drive mobile robot, which is a disc, among piecewise smooth and convex obstacles. To obtain a well-defined notion of *shortest*, the total amount of wheel rotation is optimized. We use recent characterization of minimum wheel-rotation paths for differential-drive mobile robots with no obstacles [4], [5]. We reduce the search for the shortest path to the search on a finite nonholonomic visibility graph. Edges of the graph are either minimum wheel-rotation trajectories inside the free space or trajectories on the boundary of obstacle region. Vertices of the graph are initial and goal configurations and points on the boundary of obstacle region. We call the search graph a nonholonomic visibility graph because the jump condition of the Pontryagin Maximum Principle gives a necessary condition which is reminiscent of bitangency in well-known visibility graphs. To the best of our knowledge, this is the first progress on the problem.**

I. Introduction

This paper presents a method to compute minimum wheel-rotation trajectories for differential-drive mobile robots in the plane among obstacles. By *wheel-rotation* we mean the distance travelled by the robot wheels, which is independent of the robot maximum speed. Nonholonomic shortest path problems without obstacles have been studied for some useful systems in [3], [4], [5], [8], [2], [9], [16], [19], [20], [21], [22].

The first work on shortest paths for car-like vehicles is done by Dubins [9]. He gives a characterization of time-optimal trajectories for a car with a bounded turn radius. In that problem, the car always moves forward with constant speed. He uses a purely geometrical method to characterize such shortest paths. He even studies homotopy of the space of all plane curves with bounded curvature [10]. Later, Reeds and Shepp [16] solve a similar problem in which the car is able to move backward as well. They identify 48 different shortest paths. Shortly after Reeds and Shepp, their problem is solved and also refined by Sussmann and Tang [22] with the help of optimal control techniques. Sussmann and Tang show that there are only 46 different shortest paths for Reeds-Shepp car. Souères and Laumond [20] classify the shortest paths for a Reeds-Shepp car into symmetric classes, and give the optimal control synthesis. Souères and Boissonnat [19] study the time optimality of Dubins car with angular acceleration control. They present an incomplete characterization of time-optimal trajectories for their system. However, full characterization of such time-optimal trajectories seems to be difficult because Sussmann [21] proves that there are time-optimal trajectories for that system that require infinitely many input switchings (chattering or Fuller phenomenon). Sussmann uses Zelikin and Borisov theory of chattering control [25] to prove his result. Chyba and Sekhavat [8] study time optimality for a mobile robot with one trailer. For a numerical approach to time optimality for differential-drive robots see Reister and Pin [17]. For a study on acceleration-driven mobile robots, see Renaud and Fourquet [18]. In [3], the time-optimal trajectories for the differential drive is studied, and a complete characterization of all time-optimal trajectories is given. In [2], the time-optimal trajectories for an omni-directional mobile robot is given.

Holonomic shortest path problems among obstacles have been studied in different disciplines [13], [15]. However, nonholonomic shortest path problems become harder in the presence of obstacles. For example, there are few approaches to the nonholonomic shortest path problems among obstacles [6], [23], [24]. In [6], a polynomial-time algorithm for computing a shortest path for Dubins car among moderate obstacles is given. An obstacle is said to be moderate [1] if it is convex and its boundary is a differentiable curve whose curvature is everywhere not more than 1. In [14] the problem of finding the shortest distance for Reeds-Shepp car to a manifold in configuration space is studied. In [23], [24] a method to compute the shortest distance for a car-like robot from a given configuration to the obstacle region is presented.

The approach that we use to derive optimal trajectories is similar to the visibility graph in [12], [15]. However, the difference between our method and the aforementioned method is that we construct a nonholonomic visibility graph whose edges are nonholonomic shortest paths. The obstacles are assumed to be open, bounded, disjoint, and convex subsets in the plane with a simple, piecewise-smooth with piecewise-continuous curvature boundary. The robot is a differential-drive vehicle modeled as a disc in the plane. Using the Pontryagin Jump Condition [11] we give necessary conditions for local optimality which is reminiscent of bitangency conditions in visibility-based methods. We first argue that minimum wheel-rotation

1-4244-0602-1/07/$20.00 ©2007 IEEE.

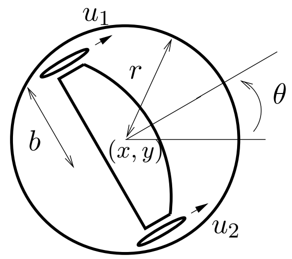

Fig. 1. The robot which is a differential-drive vehicle modeled as a disc of radius r

trajectories exist for our problem. It is then viable to apply the necessary condition of the Pontryagin Maximum Principle (PMP) and the Jump Condition [11]. We use the recent characterization of minimum wheel-rotation trajectories inside the free space [5]. Using the necessary conditions and other arguments, we restrict the search for the optimal trajectory to the search on the nonholonomic visibility graph. Any shortest path algorithm on graphs, such as Dijkstra's algorithm, can be used to extract the minimum wheel-rotation trajectory from the nonholonomic visibility graph. Some of the proofs of lemmas and propositions are omitted due to space limitations.

II. Problem Formulation

A differential-drive robot [3], [5] is a three-dimensional system with its configuration variable denoted by $q = (x, y, \theta) \in \mathcal{C} = \mathbb{R}^2 \times \mathbb{S}^1$ in which x and y are the coordinates of the point on the axle, equidistant from the wheels, in a fixed frame in the plane, and $\theta \in [0, 2\pi)$ is the angle between x-axis of the frame and the robot local longitudinal axis (see Figure 1).

The robot has independent velocity control of each wheel. Assume that the wheels have equal bounds on their velocity. More precisely, $u_1, u_2 \in [-1, 1]$, in which the inputs u_1 and u_2 are respectively the left and the right wheel velocities, and the input space is $U = [-1, 1] \times [-1, 1] \subset \mathbb{R}^2$. The system is

$$\dot{q} = f(q, u) = u_1 f_1(q) + u_2 f_2(q) \tag{1}$$

in which f_1 and f_2 are vector fields in the tangent bundle $T\mathcal{C}$ of configuration space. Let the distance between the robot wheels be $2b$, and the robot be a closed disc of radius $r > b$. In that case,

$$f_1 = \frac{1}{2}\begin{pmatrix}\cos\theta \\ \sin\theta \\ -\frac{1}{b}\end{pmatrix} \text{ and } f_2 = \frac{1}{2}\begin{pmatrix}\cos\theta \\ \sin\theta \\ \frac{1}{b}\end{pmatrix}. \tag{2}$$

The Lagrangian L and the cost functional J to be minimized are

$$L(u) = \frac{1}{2}(|u_1| + |u_2|) \tag{3}$$

$$J(u) = \int_0^T L(u(t))dt. \tag{4}$$

The factor $\frac{1}{2}$ above helps to simplify further formulas, and does not alter the optimal trajectories.

We assume that there are n obstacles, $O_1, O_2, \ldots, O_n$, in the workspace of the robot. Each O_i is a bounded, open, and convex subset of $\mathbb{R}^2$, and the boundary of O_i, which is denoted by ∂O_i, is a simple, piecewise-smooth with piecewise-continuous curvature, and closed curve. Recall that the robot is a disc of radius r. Let

$$P_i = \{p \in \mathbb{R}^2 \ \mid \ d(p, O_i) < r\}, \tag{5}$$

in which d is the Euclidean distance from a set. The obstacle region in the configuration space of the robot is

$$\mathcal{C}_{obs} = (P_1 \cup P_2 \cup \cdots \cup P_n) \times \mathbb{S}^1. \tag{6}$$

We also assume that all P_i's are disjoint. Hence

$$\partial\mathcal{C}_{obs} = (\partial P_1 \cup \partial P_2 \cup \cdots \cup \partial P_n) \times \mathbb{S}^1. \tag{7}$$

Note that P_i's are open subsets of $\mathbb{R}^2$, and hence, $\mathcal{C}_{obs}$ is open. Let $\mathcal{C}_{free} = \mathcal{C} \backslash \mathcal{C}_{obs}$ be the free part of the configuration space. Note that $\mathcal{C}_{free}$ is closed and $\partial\mathcal{C}_{free} = \partial\mathcal{C}_{obs}$. It is obvious that ∂P_i's are simple, piecewise-smooth, and closed curves.

Proposition 1. *The curvature of ∂P_i is not more than $\frac{1}{r}$ everywhere, for $i = 1, 2, \ldots, n$.*

Sketch of proof. Since O_i is convex and P_i is the set of points within distance at most r, the radius of the robot, from O_i, it is obvious that at every point $p \in \partial P_i$, a circle of radius r tangent to ∂P_i is contained in $P_i \cup \partial P_i$. This implies that the curvature of ∂P_i is not more than $\frac{1}{r}$ everywhere. ■

For every pair of free initial and goal configurations, not on the boundary of $\mathcal{C}_{free}$, we seek an admissible control, i.e. a measurable function $u : [0, T] \to U$, that minimizes J while transferring the initial configuration to the goal configuration in free region of the configuration space $\mathcal{C}_{free}$. Since the cost J is invariant by scaling the input within U, we can assume without loss of generality that the controls are either constantly zero ($u \equiv (0, 0)$) or saturated at least in one input, i.e. $\max(|u_1(t)|, |u_2(t)|) = 1$ for all $t \in [0, T]$. Since $u \equiv (0, 0)$ gives trivial motionless trajectory, we assume throughout this paper that $u \not\equiv (0, 0)$.

III. Existence of Optimal Trajectories

The differential-drive vehicle is controllable [3]. Moreover, it can be shown that the system is small-time local controllable. Hence, since the obstacles are bounded, there exists at least one trajectory between any pair of initial and goal configurations in $\mathcal{C}_{free}$, and it is meaningful to discuss the existence of optimal trajectories. Since $\mathcal{C}_{free}$ is closed, the existence of optimal trajectories follows from Filippov Existence Theorem [7] and compactification technique in [5]. For more details of the proof please refer to [5].

IV. Necessary Condition

We use previous characterization of minimum wheel-rotation trajectories [4], [5] inside free region of the configuration space, and also apply Pontryagin Jump Condition [11] which is a necessary condition for optimality of those trajectories that partially lie on the boundary of $\mathcal{C}_{free}$.

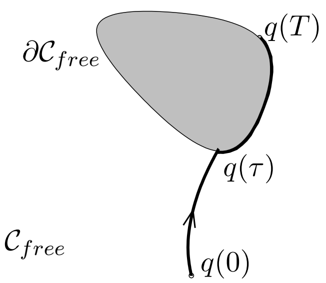

Fig. 2. The jump time τ and the jump point $q(\tau)$ on a trajectory $q(t)$

A. Pontryagin Maximum Principle (PMP) inside $\mathcal{C}_{free}$

Let the Hamiltonian $H : \mathbb{R}^3 \times \mathcal{C} \times U \to \mathbb{R}$ be

$$H(\lambda, q, u) = \langle \lambda, \dot{q} \rangle + \lambda_0 L(u) \tag{8}$$

in which λ_0 is a constant. According to the PMP [11], for every optimal trajectory $q(t)$ not touching the boundary of $\mathcal{C}_{free}$ defined on $[0, T]$ and associated with control $u(t)$, there exists a constant $\lambda_0 \leq 0$ and an absolutely continuous vector-valued adjoint function $\lambda(t)$, that is nonzero if $\lambda_0 = 0$, with the following properties along the optimal trajectory:

$$\dot{\lambda} = -\frac{\partial H}{\partial q}, \tag{9}$$

$$H(\lambda(t), q(t), u(t)) = \max_{z \in U} H(\lambda(t), q(t), z), \tag{10}$$

$$H(\lambda(t), q(t), u(t)) \equiv 0. \tag{11}$$

Let the switching functions be

$$\varphi_1 = \langle \lambda, f_1 \rangle \text{ and } \varphi_2 = \langle \lambda, f_2 \rangle, \tag{12}$$

in which f_1 and f_2 are given by (2). The analysis given in [5] proves that if $\lambda_0 = 0$ then $u \equiv (0, 0)$. We can then assume $\lambda_0 = -2$, and we have the following along $q(t)$ inside $\mathcal{C}_{free}$:

$$H = u_1\varphi_1 + u_2\varphi_2 - (|u_1| + |u_2|) \equiv 0, \tag{13}$$

$$|\varphi_i| \leq 1, \tag{14}$$

$$u_i = 0 \text{ if } |\varphi_i| < 1, \tag{15}$$

$$u_i \in [0, 1] \text{ if } \varphi_i = 1, \tag{16}$$

$$u_i \in [-1, 0] \text{ if } \varphi_i = -1, \tag{17}$$

for $i = 1, 2$ (see [5]). Moreover

$$\lambda(t) = \begin{pmatrix} \lambda_1(t) \\ \lambda_2(t) \\ \lambda_3(t) \end{pmatrix} = \begin{pmatrix} c_1 \\ c_2 \\ c_1 y - c_2 x + c_3 \end{pmatrix}, \tag{18}$$

where c_1, c_2, and c_3 are constants, and $|c_1| + |c_2| + |c_3| \neq 0$.

B. Pontryagin Jump Condition

Minimum wheel-rotation trajectories among obstacles are composed of a finite number of subpaths inside $\mathcal{C}_{free}$ and also a finite number of subpaths on the boundary of $\mathcal{C}_{free}$. In general, there can be an arbitrary number of pieces of each kind in a minimum wheel-rotation trajectory among obstacles. Throughout Section IV, we focus on a single isolated jump, i.e. those minimum wheel-rotation trajectories that have only two subpaths: one piece inside $\mathcal{C}_{free}$ and the other lying on $\partial\mathcal{C}_{free}$. In the next sections, we will address the general case.

Def 1. Let $q(t)$ be an optimal trajectory defined on $[0, T]$. Let $0 < \tau < T$ be such that $q|_{[0,\tau)}$ is inside $\mathcal{C}_{free}$ and $q|_{[\tau,T]}$ lies completely on the boundary of $\mathcal{C}_{free}$. We call τ the *jump time* of $q(t)$, and $q(\tau)$ the *jump point*. See Figure 2 for an illustration. Note that $q(t)$ is not necessarily an optimal trajectory in Figure 2.

Let H be the Hamiltonian in Section IV-A. Let

$$h(q, u) = \langle \frac{\partial m}{\partial q}, f(q, u) \rangle, \tag{19}$$

$$g(q, u) = \begin{pmatrix} g_1 \\ g_2 \\ g_3 \end{pmatrix} = \frac{\partial h}{\partial q}, \tag{20}$$

in which $m \colon \mathcal{C} \to \mathbb{R}$ is a real-valued smooth function such that the boundary of $\mathcal{C}_{free}$ is locally defined by $m(q) = 0$. Note that $\frac{\partial m}{\partial \theta} = 0$ since $\partial\mathcal{C}_{free} = (\partial P_1 \cup \partial P_2 \cup \cdots \cup \partial P_n) \times \mathbb{S}^1$. According to the PMP [11], there exists a constant $\lambda_0 \leq 0$ and vector-valued adjoint function $\lambda(t)$, that is nonzero if $\lambda_0 = 0$, with the properties in Section IV-A over the time interval $[0, \tau)$, and the following properties over the time interval $[\tau, T]$ along the optimal trajectory $q(t)$:

$$\dot{\lambda} = -\frac{\partial H}{\partial q} + c(t) g(q, u), \tag{21}$$

$$H(\lambda(t), q(t), u(t)) = \max_{z \in U} H(\lambda(t), q(t), z), \tag{22}$$

$$H(\lambda(t), q(t), u(t)) \equiv 0. \tag{23}$$

Above, $c(t)$ is a real-valued function, and $g(q, u)$ is a vector-valued function in (20). Moreover, $\lambda(t)$ is continuous on $[0, \tau)$ and $(\tau, T]$. According to the Pontryagin Jump Condition [11], at time τ one of the following two cases happen:

1) $\lambda^-(\tau) = \lambda^+(\tau)$
2) $\lambda_0 = 0$ and $\lambda^-(\tau)$ is perpendicular to the boundary of $\mathcal{C}_{free}$ at $q(\tau)$.

Above, $\lambda^-(\tau)$ and $\lambda^+(\tau)$ are the left and the right limit of $\lambda(t)$ at $t = \tau$ respectively. We may assume that the second case cannot happen because $\lambda_0 = 0$ implies $u_1 \equiv u_2 \equiv 0$. Thus, $\lambda(t)$ is continuous on the whole interval $[0, T]$. Due to the symmetries of the problem, $q(T - t)$ is an optimal trajectory if $q(t)$ is optimal. Hence, the same analysis holds if the trajectory $q(t)$ lies on the boundary of $\mathcal{C}_{free}$ over $[0, \tau]$ and is inside $\mathcal{C}_{free}$ over $(\tau, T]$.

C. Characterization of Jump Points

Let the switching functions be defined in (12). Since we showed in Section IV-B that $\lambda(t)$ is continuous along an optimal trajectory, the switching functions $\varphi_1(t)$ and $\varphi_2(t)$ are also continuous. Conditions (11) and (23) together with maximization of the Hamiltonian in (10) and (22) imply that $|\varphi_i(t)| \leq 1$, and also give the control law

$$u_i(t) \in \begin{cases} [0, 1] & \text{if} \quad \varphi_i(t) = 1 \\ \{0\} & \text{if} \quad |\varphi_i(t)| < 1 \\ [-1, 0] & \text{if} \quad \varphi_i(t) = -1 \end{cases} \tag{24}$$

along an optimal trajectory. For details of this analysis see [5].

Lemma 1. *Let $q(t)$ be an optimal trajectory defined on $[0,T]$. If τ is the jump time of $q(t)$, then $|\varphi_i(t)| = 1$ for $t \in [\tau, T]$, $i = 1, 2$. In particular, $|\varphi_i(\tau)| = 1$.*

Proof. Suppose $|\varphi_i(t_0)| < 1$ for some $t_0 \in [\tau, T]$ and some $i = 1, 2$. Let j be the index of obstacle, i.e. $(x(t_0), y(t_0)) \in \partial P_j$ where $q(t_0) = (x(t_0), y(t_0), \theta(t_0))$. Since $\varphi_i(t)$ is continuous on $[0,T]$, there exists $\epsilon > 0$ such that $|\varphi_i(t)| < 1$ for $t \in [t_0 - \epsilon, t_0 + \epsilon]$. Thus, the control law (24) implies that the robot swings over the interval $[t_0 - \epsilon, t_0 + \epsilon]$, i.e. $u_i|_{[t_0-\epsilon, t_0+\epsilon]} = 0$. This is impossible because by Proposition 1, the curvature of ∂P_j does not exceed $\frac{1}{r}$, and center of the robot follows a circle of radius b while swinging. The curvature of this circle is $\frac{1}{b} > \frac{1}{r}$. Thus, the robot cannot follow the boundary of $\mathcal{C}_{free}$ at $(x(t_0), y(t_0))$ while swinging. ∎

Def 2. Let $q(t)$ be an optimal trajectory defined on $[0,T]$ associated with adjoint $\lambda(t)$. Let $\tau \in [0,T]$ be its jump time. In Section IV-A, we showed that $\lambda(t)$ is given by (18) for $t \in [0, \tau)$. Let c_1, c_2, and c_3 be the constants in (18). We call $q(t)$ a *loose* optimal trajectory if $c_1 = c_2 = 0$ and $|c_3| = 2b$. We call $q(t)$ a *tight* optimal trajectory if $|c_1| + |c_2| \neq 0$.

According to [5], minimum wheel-rotation trajectories inside $\mathcal{C}_{free}$ are either tight or loose.

D. Jump Points of Tight Optimal Trajectories

Lemma 2. *Let $q(t)$ be a tight optimal trajectory defined on $[0,T]$. If τ is the jump time of $q(t)$, then either $\varphi_1(t) = \varphi_2(t) = 1$ or $\varphi_1(t) = \varphi_2(t) = -1$ for $t \in [\tau, T]$.*

Proof. Lemma 1 shows that $|\varphi_1(t)| = |\varphi_2(t)| = 1$ for $t \in [\tau, T]$. Since $\varphi_i(t)$'s are continuous over $[0,T]$, it is enough to show that $\varphi_1(\tau) = \varphi_2(\tau)$. On the contrary, if $\varphi_1(\tau) = -\varphi_2(\tau)$, control law (24) implies $u_1(\tau)u_2(\tau) \leq 0$. Since $\varphi_i(t)$'s are continuous, there exists $\epsilon > 0$ such that $u_1(t)u_2(t) \leq 0$ for $t \in [\tau, \tau+\epsilon]$. Furthermore, $u_1(t) = -u_2(t)$ for $t \in [\tau, \tau + \epsilon]$, because otherwise center of the robot traverses a path in the plane with curvature more than $\frac{1}{r}$, which does not lie on the boundary of $\mathcal{C}_{free}$ by Proposition 1. Thus, the robot rotates in place over the interval $[\tau, \tau + \epsilon]$, i.e. $u_1(t) = -u_2(t)$, and over this interval

$$g_1(q,u) = \frac{u_1 + u_2}{2}\left(\frac{\partial^2 m}{\partial x^2}\cos\theta + \frac{\partial^2 m}{\partial x \partial y}\sin\theta\right) \equiv 0, \qquad (25)$$

$$g_2(q,u) = \frac{u_1 + u_2}{2}\left(\frac{\partial^2 m}{\partial y \partial x}\cos\theta + \frac{\partial^2 m}{\partial y^2}\sin\theta\right) \equiv 0, \qquad (26)$$

in which $g(q,u)$ is defined in (20). Consequently, (21) implies that $\dot{\lambda}_1 \equiv \dot{\lambda}_2 \equiv 0$ and $\lambda_1(t) \equiv c_1$, $\lambda_2(t) \equiv c_2$, for constants c_1 and c_2, over the interval $[\tau, \tau + \epsilon]$. Since $q(t)$ is assumed to be tight, $|c_1| + |c_2| \neq 0$. Finally $\varphi_1(t) = -\varphi_2(t)$ implies $c_1 \cos\theta + c_2 \sin\theta \equiv 0$ over the interval $[\tau, \tau + \epsilon]$. This is true only if $\dot{\theta} \equiv 0$, which is contradiction. ∎

Lemma 3. *Let $q(t)$ be a tight optimal trajectory defined on $[0,T]$. If τ is the jump time of $q(t)$, and $(x(\tau), y(\tau)) \in \partial P_j$, then the vector $(\cos\theta(\tau), \sin\theta(\tau))$ is tangent to ∂P_j at $(x(\tau), y(\tau))$.*

Proof. By Lemma 2, $\varphi_1(t) = \varphi_2(t)$ over the interval $[\tau, T]$. Thus, control law (24) implies $u_1(\tau)u_2(\tau) \geq 0$, i.e. the robot cannot rotate in place. Since $\dot{q}(\tau)$ is tangent to $\partial P_j \times \mathbb{S}^1$ at $q(\tau)$, and $(\dot{x}(\tau), \dot{y}(\tau)) = ((u_1 + u_2)/2)(\cos\theta(\tau), \sin\theta(\tau)) \neq (0,0)$, the vector $(\cos\theta(\tau), \sin\theta(\tau))$ is tangent to ∂P_j at $(x(\tau), y(\tau))$. ∎

Lemma 3 proves that the robot joins the boundary of an obstacle region tangentially from inside $\mathcal{C}_{free}$ over a tight optimal trajectory. Equivalently, the robot leaves the boundary of an obstacle region tangentially to move inside $\mathcal{C}_{free}$ over a tight optimal trajectory. In other words, orientation of the robot is tangent to the obstacle region at the jump point.

Lemma 4. *Let $q(t)$ be a tight optimal trajectory defined on $[0,T]$. If τ is the jump time of $q(t)$, then $\lambda_3(\tau) = c_1 y(\tau) - c_2 x(\tau) + c_3 = 0$.*

Proof. By Lemma 2, $\varphi_1(\tau) = \varphi_2(\tau)$. Equations (2), (12), and (18) give the result. ∎

In [5], a geometric representation of the tight minimum-wheel rotation trajectories inside $\mathcal{C}_{free}$ is given. According to that representation, Lemma 4 shows that center of the robot lies on the center line of region $S_{\pm}$, defined by $c_1 y - c_2 x + c_3 = 0$, at the jump point.

E. Jump Points of Loose Optimal Trajectories

Lemma 5. *Let $q(t)$ be a loose optimal trajectory defined on $[0,T]$. If τ is the jump time of $q(t)$, then either $\varphi_1(t) = -\varphi_2(t) = 1$ or $\varphi_1(t) = -\varphi_2(t) = -1$ for $t \in [\tau, T]$. Moreover, $u_1(t) = -u_2(t)$ for $t \in [\tau, T]$. In other words, the robot rotates in place over the interval $[\tau, T]$.*

Proof. Lemma 1 shows that $|\varphi_1(t)| = |\varphi_2(t)| = 1$ for $t \in [\tau, T]$. Since $\varphi_i(t)$'s are continuous over $[0,T]$, it is enough to show that $\varphi_1(\tau) = -\varphi_2(\tau)$. Since $q(t)$ is loose, $c_1 = c_2 = 0$ and $|c_3| = 2b$. Equations (2) , (12), and (18) show that $\varphi_1(\tau) = -\frac{c_3}{2b}$ and $\varphi_2(\tau) = \frac{c_3}{2b}$. Control law (24) shows that $u_1(t)u_2(t) \leq 0$ for $t \in [\tau, T]$. Furthermore, if there exist $\epsilon > 0$ and $t_0 \in [\tau, T - \epsilon]$ such that $u_1(t) \neq -u_2(t)$ for $t \in [t_0, t_0 + \epsilon]$, then center of the robot traverses a path in the plane with curvature more than $\frac{1}{r}$, which does not lie on the boundary of $\mathcal{C}_{free}$ by Proposition 1. ∎

Lemma 6. *Let $q(t)$ be a loose optimal trajectory defined on $[0,T]$. If τ is the jump time of $q(t)$, then $\lambda_1(t) = 0$, $\lambda_2(t) = 0$, and $|\lambda_3(t)| = 2b$ for $t \in [0,T]$.*

Proof. By Lemma 5 the robot rotates in place over the interval $[\tau, T]$, i.e. $u_1(t) = -u_2(t)$, and over this interval

$$g_1(q,u) = \frac{u_1 + u_2}{2}\left(\frac{\partial^2 m}{\partial x^2}\cos\theta + \frac{\partial^2 m}{\partial x \partial y}\sin\theta\right) \equiv 0, \qquad (27)$$

$$g_2(q,u) = \frac{u_1 + u_2}{2}\left(\frac{\partial^2 m}{\partial y \partial x}\cos\theta + \frac{\partial^2 m}{\partial y^2}\sin\theta\right) \equiv 0, \qquad (28)$$

in which $g(q,u)$ is defined in (20). Consequently, (21) implies that $\dot{\lambda}_1 \equiv \dot{\lambda}_2 \equiv 0$ and $\lambda_1(t) = 0$, $\lambda_2(t) = 0$ over the interval

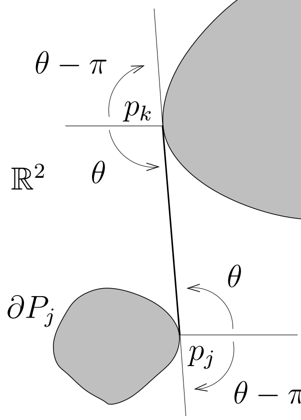

Fig. 3. An illustration of bitangent edges (v_j^1, v_k^1) and (v_j^2, v_k^2) in the nonholonomic visibility graph $\mathbf{G}$, in which $v_j^1 = (p_j, \theta), v_j^2 = (p_j, \theta - \pi) \in \mathbb{R}^2 \times \mathbb{S}^1$ and $v_k^1 = (p_k, \theta), v_k^2 = (p_k, \theta - \pi) \in \mathbb{R}^2 \times \mathbb{S}^1$

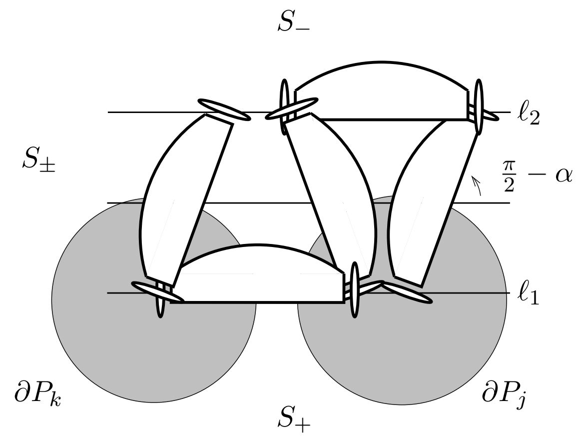

Fig. 4. Illustration of $\mathbf{R}_{\frac{\pi}{2}-\alpha}\mathbf{L}_{\frac{\pi}{2}-\alpha}\mathbf{R}_{\frac{\pi}{2}-\alpha}\mathbf{L}_{\frac{\pi}{2}-\alpha}$ as an edge of $\mathbf{G}$. Note that $S_\pm$ width is less than $2b$ in this case.

$[0, T]$. Finally, $|\lambda_3(t)| = 2b$ over the interval $[0, T]$, because otherwise $|\varphi_i(t)| \neq 1$. ■

Due to symmetries of the problem, there is no difference between the case where the trajectory joins the boundary of obstacle region from inside $\mathcal{C}_{free}$ and the case where the trajectory leaves the boundary of obstacle region to move inside $\mathcal{C}_{free}$. Lemma 6 shows that a loose optimal trajectory remains loose all over the time interval. In other words, if any subpath of an optimal trajectory is loose, then the whole trajectory is loose. In [5] loose minimum wheel-rotation trajectories are completely characterized. In particular Lemmas 6 and 7 of [5] hold for the case of loose optimal trajectories among obstacles. Following notation of [5], denote rotation in place by $\mathbf{P}$, straight segment by $\mathbf{S}$, and swing around the left and the right wheel by $\mathbf{L}$ and $\mathbf{R}$ respectively. Subscripts here denote the length. Thus, loose optimal trajectories among obstacles are composed of a sequence of rotation in place and swing segments, and are of the form $\mathbf{R}_\alpha\mathbf{P}_{\pi-\gamma}\mathbf{L}_\gamma\mathbf{P}_{\pi-\gamma}\mathbf{R}_\gamma \cdots \mathbf{P}_{\pi-\gamma}\mathbf{L}_\beta$ or $\mathbf{R}_\alpha\mathbf{P}_{\pi-\gamma}\mathbf{L}_\gamma\mathbf{P}_{\pi-\gamma}\mathbf{R}_\gamma \cdots \mathbf{P}_{\pi-\gamma}\mathbf{R}_\beta$ for $0 \leq \alpha, \beta \leq \gamma \leq \pi$.

V. Nonholonomic Visibility Graph

In previous section we focused on a single jump on an optimal trajectory. In Lemma 3 we showed that orientation vector of the robot is tangent to the boundary of obstacle region at a jump point over a tight optimal trajectory. In Lemma 4 we showed that center of the robot lies on the center line of $S_\pm$ region (see [5]) at a jump point over a tight optimal trajectory. Also, there are no differences between the case where the trajectory joins the boundary of obstacle region from inside $\mathcal{C}_{free}$ and the case where the trajectory leaves the boundary of obstacle region to move inside $\mathcal{C}_{free}$. We also characterized loose optimal trajectories in Section IV-E.

We define a nonholonomic visibility graph $\mathbf{G} = (\mathbf{V}, \mathbf{E})$ among the obstacle regions $P_1, P_2, \ldots, P_n$. Vertices are configurations in $\mathbb{R}^2 \times \mathbb{S}^1$, i.e $\mathbf{V} \subset \mathcal{C}_{free}$. At each vertex of $\mathbf{G}$ that lies on $\partial\mathcal{C}_{free}$, orientation of the robot is tangent to the boundary of obstacle region. Thus, there are at most two choices for the orientation of every vertex in $\mathbf{V}$. When both orientations exist in the graph, the two vertices are distinct and there is no edge between them in $\mathbf{G}$.

Lemma 3 shows the orientation vector of the robot is tangent to the obstacle boundary at a jump point on a tight minimum wheel-rotation piece. Lemma 4 proves that a jump point along a tight minimum wheel-rotation piece lies on the centerline of $S_\pm$ region.

In order to construct $\mathbf{G}$, first add all free bitangent line segments between any ∂P_j and ∂P_k to $\mathbf{G}$. In particular, if $p_j \in \partial P_j$ and $p_k \in \partial P_k$, then $v_j^1 = (p_j, \theta), v_j^2 = (p_j, \theta - \pi), v_k^1 = (p_k, \theta), v_k^2 = (p_k, \theta - \pi) \in \mathbf{V}$ and $(v_j^1, v_k^1), (v_j^2, v_k^2) \in \mathbf{E}$ if the line segment $p_j - p_k$ is tangent to ∂P_j at p_j and tangent to ∂P_k at p_k and is completely in $\mathcal{C}_{free}$. Associate the length of $p_j - p_k$ segment to the edges (v_j^1, v_k^1) and (v_j^2, v_k^2) in $\mathbf{G}$. Add edge (v_j^1, v_k^2) (and (v_j^2, v_k^1)) to $\mathbf{G}$ if there is a trajectory $\mathbf{S}_{d_1}\mathbf{L}_{\frac{\pi}{2}}\mathbf{S}_{d_2}\mathbf{R}_{\frac{\pi}{2}}\mathbf{S}_{d_3}$ or $\mathbf{S}_{d_1}\mathbf{R}_{\frac{\pi}{2}}\mathbf{S}_{d_2}\mathbf{L}_{\frac{\pi}{2}}\mathbf{S}_{d_3}$ which starts at v_j^1 (respectively v_j^2) and ends at v_k^2 (respectively v_k^1) and is completely in $\mathcal{C}_{free}$. Note that the swing parts of such trajectories are in the same direction, i.e. both clockwise or both counter-clockwise. Associate wheel rotation of the trajectory which is $d_1 + d_2 + d_3 + \pi$ to the edges (v_j^1, v_k^2) and (v_j^2, v_k^1). Note that the vector of orientation of the robot $(\cos\theta, \sin\theta)$ is tangent to ∂P_j at p_j and tangent to ∂P_k at p_k. The superscripts of v^1, v^2 represent two different orientations which are an angle π apart. See Figure 3 for an illustration. This construction corresponds to those tight minimum wheel-rotation pieces for which the width of $S_\pm$ region is $2b$ (see [5]).

Second, add to $\mathbf{G}$ all of the free segments between any ∂P_j and ∂P_k that make equal angle with the tangent. More precisely, if $p_j \in \partial P_j$ and $p_k \in \partial P_k$, then $v_j = (p_j, \theta_j), v_k = (p_k, \theta_k) \in \mathbf{V}$ and $(v_j, v_k) \in \mathbf{E}$ if the angle α between the segment $p_j - p_k$ and the tangent on ∂P_j at p_j is equal to the angle between the segment $p_j - p_k$ and the tangent on ∂P_k at p_k, and one of the paths $\mathbf{R}_{\frac{\pi}{2}-\alpha}\mathbf{L}_{\frac{\pi}{2}-\alpha}$, $\mathbf{L}_{\frac{\pi}{2}-\alpha}\mathbf{R}_{\frac{\pi}{2}-\alpha}$, $\mathbf{R}_{\frac{\pi}{2}-\alpha}\mathbf{L}_{\frac{\pi}{2}-\alpha}\mathbf{R}_{\frac{\pi}{2}-\alpha}\mathbf{L}_{\frac{\pi}{2}-\alpha}$, or $\mathbf{L}_{\frac{\pi}{2}-\alpha}\mathbf{R}_{\frac{\pi}{2}-\alpha}\mathbf{L}_{\frac{\pi}{2}-\alpha}\mathbf{R}_{\frac{\pi}{2}-\alpha}$ which takes the robot from v_j to v_k is completely in $\mathcal{C}_{free}$. In such trajectories the first two swings are in the same direction and the remaining two are also in the same direction, i.e. both clockwise or both counter-clockwise (see [5]). This construction corresponds to those tight minimum wheel-rotation pieces for which the width of $S_{\pm}$ region is less than $2b$. See Figure 4 for an illustration. Associate wheel rotation of such path which is $\pi - 2\alpha$ or $2\pi - 4\alpha$ to the edge (v_j, v_k).

Finally, add initial and goal configurations, v_{init} and v_{goal}, to $\mathbf{V}$. If the minimum wheel-rotation trajectory between v_{init} and v_{goal} is in $\mathcal{C}_{free}$, then add the edge (v_{init}, v_{goal}) to $\mathbf{E}$ and we are done. Also check if there exists any loose trajectory of the form given in Section IV-E between v_{init} and v_{goal}. If $p_j \in \partial P_j$, then $v_j = (p_j, \theta_j) \in \mathbf{V}$ and $(v_{init}, v_j) \in \mathbf{E}$ if there exists a tight minimum wheel-rotation trajectory of type I or type II (see [5]) which takes the robot from v_{init} to v_j and is completely inside $\mathcal{C}_{free}$. Associate wheel rotation of such path to this edge. Again, orientation of the robot at v_j is tangent to ∂P_j at p_j. Do the same for (v_j, v_{goal}). Eventually, for every pair $v_1 = (p_1, \theta_1), v_2 = (p_2, \theta_2) \in \mathbf{V}$ such that p_1 and p_2 belong to the same boundary component ∂P_ℓ, add an edge $(v_1, v_2) \in \mathbf{E}$ if the robot can move from v_1 to v_2 by following the boundary of obstacle ∂P_ℓ. Associate the length of the path in ∂P_ℓ to this edge.

VI. Computing The Optimal Trajectory

In previous section we construct the nonholonomic visibility graph $\mathbf{G}$. The initial and goal configurations v_{init} and v_{goal} are two vertices in $\mathbf{G}$, and all other vertices in $\mathbf{G}$ are configurations in $\partial\mathcal{C}_{free}$. Between every two adjacent vertices in $\mathbf{G}$ there exists a collision-free trajectory. By the analysis given in Section IV the minimum wheel-rotation trajectory between the initial and goal configurations lies on $\mathbf{G}$. In other words, the minimum wheel-rotation trajectory between the initial and goal configurations is a path in $\mathbf{G}$ from v_{init} to v_{goal}. Thus, by using a standard shortest path algorithm such as Dijkstra's algorithm on the finite graph $\mathbf{G}$, the minimum wheel-rotation trajectory between the initial and goal configurations can be extracted.

VII. Conclusions

We first argue that minimum wheel-rotation trajectories exist for this problem. By using previous characterization of minimum wheel-rotation trajectories inside the free space [4], [5], the Pontryagin Jump Condition [11], and other methods we give necessary conditions for optimality. Necessary conditions help to restrict the search for the optimal trajectory to a nonholonomic visibility graph which is constructed. Using any shortest path algorithm on graphs, such as Dijkstra's algorithm, the minimum wheel-rotation trajectory between the initial and goal configurations can be extracted.

References

[1] P. K. Agarwal, P. Raghavan, and H.Tamaki. Motion planning for a steering constrained robot through moderate obstacles. In *Proc. ACM Symposium on Computational Geometry*, pages 343–352, 1995.

[2] Devin J. Balkcom, Paritosh A. Kavathekar, and Matthew T. Mason. The minimum-time trajectories for an omni-directional vehicle. In *Proc. Sixth International Workshop on the Algorithmic Foundations of Robotics*, 2006.

[3] Devin J. Balkcom and Matthew. T. Mason. Time optimal trajectories for bounded velocity differential drive vehicles. *Int. J. Robot. Res.*, 21(3):199–218, March 2002.

[4] H. Chitsaz, S.M. LaValle, D.J. Balkcom, and M.T. Mason. An explicit characterization of minimum wheel-rotation paths for differential-drives. In *IEEE International Conference on Methods and Models in Automation and Robotics*, 2006.

[5] H. Chitsaz, S.M. LaValle, D.J. Balkcom, and M.T. Mason. Minimum wheel-rotation paths for differential-drive mobile robots. In *IEEE International Conference on Robotics and Automation*, 2006.

[6] J. D. Boissonnat and S. Lazard. A polynomial-time algorithm for computing a shortest path of bounded curvature amidst moderate obstacles. In *Proc. ACM Symposium on Computational Geometry*, pages 242–251, 1996.

[7] Lamberto Cesari. *Optimization Theory and Applications: problems with ordinary differetial equations*. Springer-Verlag, New York, NY, 1983.

[8] M. Chyba and S. Sekhavat. Time optimal paths for a mobile robot with one trailer. In *IEEE/RSJ Int. Conf. on Intelligent Robots & Systems*, volume 3, pages 1669–1674, 1999.

[9] L. E. Dubins. On curves of minimal length with a constraint on average curvature, and with prescribed initial and terminal positions and tangents. *American Journal of Mathematics*, 79:497–516, 1957.

[10] L. E. Dubins. On plane curves with curvature. *Pacific J. Math.*, 11(2):471–481, 1961.

[11] L.S. Pontryagin, V.G. Boltyanskii, R.V. Gamkrelidze, and E.F. Mishchenko. *The Mathematical Theory of Optimal Processes*. John Wiley, 1962.

[12] T. Lozano-Pérez and M. A. Wesley. An algorithm for planning collision-free paths among polyhedral obstacles. *Communications of the ACM*, 22(10):560–570, 1979.

[13] J. S. B. Mitchell. Shortest paths and networks. In J. E. Goodman and J. O'Rourke, editors, *Handbook of Discrete and Computational Geometry, 2nd Ed.*, pages 607–641. Chapman and Hall/CRC Press, New York, 2004.

[14] P. Moutarlier, B. Mirtich, and J. Canny. Shortest paths for a car-like robot to manifolds in configuration space. *Int. J. Robot. Res.*, 15(1), 1996.

[15] N. J. Nilsson. A mobile automaton: An application of artificial intelligence techniques. In *1st International Joint Conference on Artificial Intelligence*, pages 509–520, 1969.

[16] J. A. Reeds and L. A. Shepp. Optimal paths for a car that goes both forwards and backwards. *Pacific J. Math.*, 145(2):367–393, 1990.

[17] David B. Reister and Francois G. Pin. Time-optimal trajectories for mobile robots with two independently driven wheels. *International Journal of Robotics Research*, 13(1):38–54, February 1994.

[18] M. Renaud and J.Y. Fourquet. Minimum time motion of a mobile robot with two independent acceleration-driven wheels. In *IEEE International Conference on Robotics and Automation*, pages 2608–2613, 1997.

[19] P. Souères and J.-D. Boissonnat. Optimal trajectories for nonholonomic mobile robots. In J.-P. Laumond, editor, *Robot Motion Planning and Control*, pages 93–170. Springer, 1998.

[20] P. Souères and J. P. Laumond. Shortest paths synthesis for a car-like robot. In *IEEE Transactions on Automatic Control*, pages 672–688, 1996.

[21] Héctor Sussmann. The markov-dubins problem with angular acceleration control. In *Proccedings of the 36th IEEE Conference on Decision and Control, San Diego, CA*, pages 2639–2643. IEEE Publications, 1997.

[22] Héctor Sussmann and Guoqing Tang. Shortest paths for the Reeds-Shepp car: A worked out example of the use of geometric techniques in nonlinear optimal control. Technical Report SYNCON 91-10, Dept. of Mathematics, Rutgers University, 1991.

[23] M. Vendittelli, J.P. Laumond, and C. Nissoux. Obstacle distance for car-like robots. *IEEE Transactions on Robotics and Automation*, 15(4):678–691, 1999.

[24] M. Vendittelli, J.P. Laumond, and P. Souères. Shortest paths to obstacles for a polygonal car-like robot. In *IEEE Conf. Decision & Control*, 1999.

[25] M.I. Zelikin and V.F. Borisov. *Theory of Chattering Control*. Birkhäuser, Boston, NJ, 1994.